ApJ, submitted
Preprint typeset using LaTeX style emulateapj v. 25/04/01

THE OPTICAL LUMINOSITY FUNCTION OF VIRIALIZED SYSTEMS

Christian MARINONI
Department of Astronomy, Cornell University, Ithaca, NY
Dipartimento di Astronomia, Università degli Studi di Trieste, Trieste, Italy
marinoni@astrosun.tn.cornell.edu

Michael J. HUDSON
Dept. of Physics, University of Waterloo, Waterloo, Canada
mjhudson@astro.uwaterloo.ca

Giuliano GIURICIN [1]
Dipartimento di Astronomia, Università degli Studi di Trieste, Trieste
SISSA, Trieste, Italy
ApJ, submitted

ABSTRACT

We determine the optical luminosity function of virialized systems over the full range of density enhancements, from single galaxies to clusters of galaxies. The analysis is based on galaxy systems identified from the Nearby Optical Galaxy (NOG) sample, which is the largest, all-sky catalog of objectively-identified bound objects presently available.

We find that the B-band luminosity function of systems is insensitive to the choice of the group-finding algorithms and is well described, over the absolute-magnitude range $-24.5 \leq M + 5\log h_{75} \leq -18.5$, by a Schechter function with $\alpha_{\rm s} = -1.4 \pm 0.03$, $M^*_{\rm s} - 5\log h_{75} = -23.1 \pm 0.06$ and $\phi^*_{\rm s} = 4.8 \times 10^{-4}\ h^3_{75}\ {\rm Mpc}^{-3}$ or by a double power law: $\phi_{\rm pl}(L_{\rm s}) \propto L_{\rm s}^{-1.45\pm0.07}$ for $L_{\rm s} < L_{\rm pl}$ and $\phi(L_{\rm s}) \propto L_{\rm s}^{-2.35\pm0.15}$ for $L_{\rm s} > L_{\rm pl}$ with $L_{\rm pl} = 8.5 \times 10^{10} h^{-2}_{75} L_\odot$, corresponding to $M_{\rm s} - 5\log h_{75} = -21.85$. The characteristic luminosity of virialized systems, $L_{\rm pl}$, is ~ 3 times brighter than that ($L^*_{\rm gal}$) of the luminosity function of NOG galaxies. Our results show that half of the luminosity of the universe is generated in systems with $L_{\rm s} < 2.9 L^*_{\rm gal}$ and that 10% of the overall luminosity density is supplied by systems with $L_{\rm s} > 30 L^*_{\rm gal}$.

We find a significant environmental dependence in the luminosity function of systems, in the sense that overdense regions, as measured on scales of $5h^{-1}$ Mpc, preferentially host brighter, and presumably more massive, virialized systems.

Subject headings: cosmology: large-scale structure of the universe — galaxies: clusters: general — galaxies: halos — galaxies: luminosity function

1. INTRODUCTION

From a theoretical perspective, dark matter halos are the basic building blocks of the structure in the Universe. Observationally, halos must be identified with virialized galaxy "systems", ranging from single dwarf galaxies to rich clusters of galaxies. The missing link between the two is the mass-to-light ratio, which in general is a function of mass or luminosity. As a first step toward understanding this relationship, in this paper we determine the luminosity function, not of individual galaxies, but of entire virialized systems. This can be compared with the luminosity functions theoretically predicted by semi-analytic models of galaxy formation and with other halo statistics (Marinoni & Hudson 2001), such as the mass function.

While the luminosity function (LF) of cluster and group galaxies has been extensively studied in literature (Iovino et al. 1993; Marzke & da Costa 1997; Lumsden et al. 1997; Gaidos 1997; Rauzy, Adami, & Mazure 1998; Bromley et al. 1998; Ramella et al. 1999; Marinoni et al. 1999), only few detailed studies have examined the LF of galaxy systems. Gott & Turner (1977, GT) used data for 103 groups identified in two dimensions (i.e. from the angular coordinates of galaxies only) to determine the functional shape of the observed group LF. Bahcall (1979), combining the GT data with the Abell (1958) clusters, attempted to extrapolate the observed luminosity distribution into the rich-cluster domain. These early studies, however, suffered from a number of weaknesses: groups identified only in projection on the sky, small-number statistics, and uncertain completeness and corrections. These weaknesses were largely overcome by MFW, who determined the LF of systems using 163 groups (with ≥ 3 members) identified in the CfA1 redshift survey (Davis et al. 1982; Huchra et al. 1983), the best data set available at that time. The quality and quantity of the data have improved considerably since those studies, allowing a more robust determination of the LF of virialized systems (hereafter VSLF).

Our VSLF is based on the Nearby Optical Galaxy (NOG) catalog (Marinoni 2001), a nearly all-sky, complete, magnitude-limited sample of $\sim$ 7000 bright and nearby galaxies. In order to assess the effects of grouping algorithms, we will analyze three catalogs of groups, all based on NOG but extracted using different algorithms and selection criteria (Giuricin et al. 2000). When grouped, NOG contains $\sim$2800 isolated galaxies and $\sim$ 1100 systems ($\sim$600 binaries and $\sim$500 groups with at least

[1] Deceased.

three members). This group catalog combines a representative volume ($cz < 6000$ km s^{-1}, nearly all-sky) of the Universe with a high comoving density of galaxies to allow excellent statistics in the group regime.

This paper is the fifth in a series (Marinoni et al. 1998, Paper I; Marinoni et al. 1999, Paper II; Giuricin et al. 2000, Paper III; Giuricin et al. 2001, Paper IV;) in which we investigate the properties of the large-scale structures as traced by the NOG sample. The outline of our paper is as follows: in §2 we review and summarize the identification procedures of NOG galaxy systems and discuss some specific properties of NOG groups. In §3 we describe our method for calculating the VSLF and apply it to our sample. Results are summarized in §4.

Throughout this paper, the Hubble constant is taken to be 75 h_{75} km s^{-1} Mpc^{-1} and the recession velocities $cz_{\rm LG}$ are evaluated in the Local Group rest frame.

2. THE NOG GROUPS: IDENTIFICATION AND SPATIAL DISTRIBUTION

The NOG sample is a statistically controlled, distance-limited ($cz_{\rm LG} \leq 6000$km s^{-1}) and magnitude-limited ($B \leq 14$) complete sample of more than 7000 optical galaxies. The sample covers 2/3 (8.27 sr) of the sky ($|b| > 20°$), a volume of $1.41 \times 10^6 h_{75}^3$ Mpc^{-3} and has a redshift completeness of 98% (see Marinoni 2001). In this paper we use the small extension of the NOG (for a total of 7232 galaxies) containing 156 additional galaxies which have rough estimates of magnitudes (see Paper III for details). Note that, in contrast to most previous studies of large-scale structure, the magnitudes used in this paper are homogenized total blue magnitudes, given in the standard system of the RC3 catalog (de Vaucouleurs et al. 1991) and fully corrected for Galactic and internal extinction and K-dimming.

Redshift maps present two principal distortions: i) small-scale perturbations caused by random velocities in clusters of galaxies which produce the so-called "Fingers of God" i.e. a radial stretching in galaxy maps pointed at the observer and ii) large-scale perturbations caused by large overdensities leading to coherent *bulk* motions. For the purposes of this paper, the latter effect of large-scale peculiar velocities are not severe; these can be easily treated via the flow models derived in Paper I.

We corrected for the Finger-of-God effect in Paper III, where galaxy systems were identified by means of different objective, group-finding algorithms i.e. the widely-used hierarchical (H) and percolation (P) (or *friends-of-friends*) algorithms. The P algorithm (Huchra & Geller 1982) identifies as members of galaxy aggregations the galaxies which have their transverse separation $D_{ij} \leq D_0 \cdot R$ and line-of-sight velocity difference $cz_{ij} \leq cz_0 \cdot R$, where R is a scaling parameter which takes into account the decrease of the magnitude range of the luminosity function sampled at increasing distance. In Paper III, two variants of the percolation method were used to identify groups. In one variant (hereafter denoted as "scaled" friends-of-friends or P2, following Paper III), typical values for the linking parameters, at the median depth of the sample (~ 4000 km s^{-1}), are 434 km s^{-1} in velocity and 0.89 ${h_{75}}^{-1}$ Mpc in transverse separation, and both link parameters were then suitably scaled with distance to give a density threshold of $\frac{\delta n}{n} = 80$. In the other variant (hereafter denoted simply as percolation or P1), only the transverse separation link parameter was scaled with distance, while the velocity link parameter was fixed at the value of 350 km s^{-1}. Given the limited range of redshift encompassed by the NOG, this choice was used to approximate a slow scaling of the velocity link parameter with distance, as suggested by cosmological N-body simulations (e.g., Nolthenius & White 1987).

The hierarchical clustering method introduced by Materne (1978) and revised by Tully (1980) is an algorithm which generates a hierarchical sequence of systems organized by some *affinity* parameter. In paper III, the authors adopted $\rho_L = 8 \times 10^9 L_\odot$ Mpc^{-3} (corresponding to a luminosity density contrast $\frac{\delta\rho_L}{\rho_L} = 45$) as the limiting luminosity density parameter used for cutting the hierarchy and defining groups.

For both algorithms, the adopted values of the group-selection parameters were chosen after a search in the parameter space guided by numerical simulations in order to obtain realistic and homogeneous catalogs of groups. Since all three catalogs are based on the same galaxy sample, this allows us to investigate systematic effects related to the choice of grouping algorithm.

Most of the NOG galaxies (∼60%) are found to be members of galaxy binaries (which comprise ∼15% of galaxies) or groups with at least three members (∼45% of galaxies). About 40% of the galaxies are left ungrouped (isolated galaxies).

In Paper III, the similarity between the catalogs of groups was demonstrated using the fraction of members in common to groups of different catalogs. In this paper, we also show that the three catalogs of groups show similar statistical distributions and trace similar large-scale structures. Figure 1 shows the distributions of P2 groups on the sky. The smoothed group number density contrast at a given point $\mathbf{r}$ (in units of velocity) has been computed by summing the contribution from all the i groups of our catalog:

$$\frac{\delta n}{n}(\mathbf{r}, R_{\rm s}) = \frac{1}{n} \sum_i \frac{W\left(\frac{|\mathbf{r}-\mathbf{r}_i|}{R_{\rm s}}\right)}{S(r_i)} - 1 \qquad (1)$$

where

$$n = \frac{1}{V} \sum_i S(\mathbf{r}_i)^{-1} \qquad (2)$$

$$W\left(\frac{|\mathbf{r}|}{R_{\rm s}}\right) = \frac{1}{(2\pi R_{\rm s}^2)^{3/2}} e^{-\frac{r^2}{2R_{\rm s}^2}} \qquad (3)$$

$$S(r) = \frac{\int_{-\infty}^{m_{\rm lim}-5\log r-15} \phi(M) dM}{\int_{-\infty}^{\infty} \phi(M) dM} \qquad (4)$$

are the mean number density, smoothing and selection functions respectively, and where $m_{\rm lim} = 12$ is the limiting apparent magnitude of completeness of the group catalog (see §3.2). Smoothing is performed in three dimensions with a variable Gaussian smoothing length $R_{\rm s}$ given by the mean inter-group separation ranging from 300 to 670 km s^{-1}.

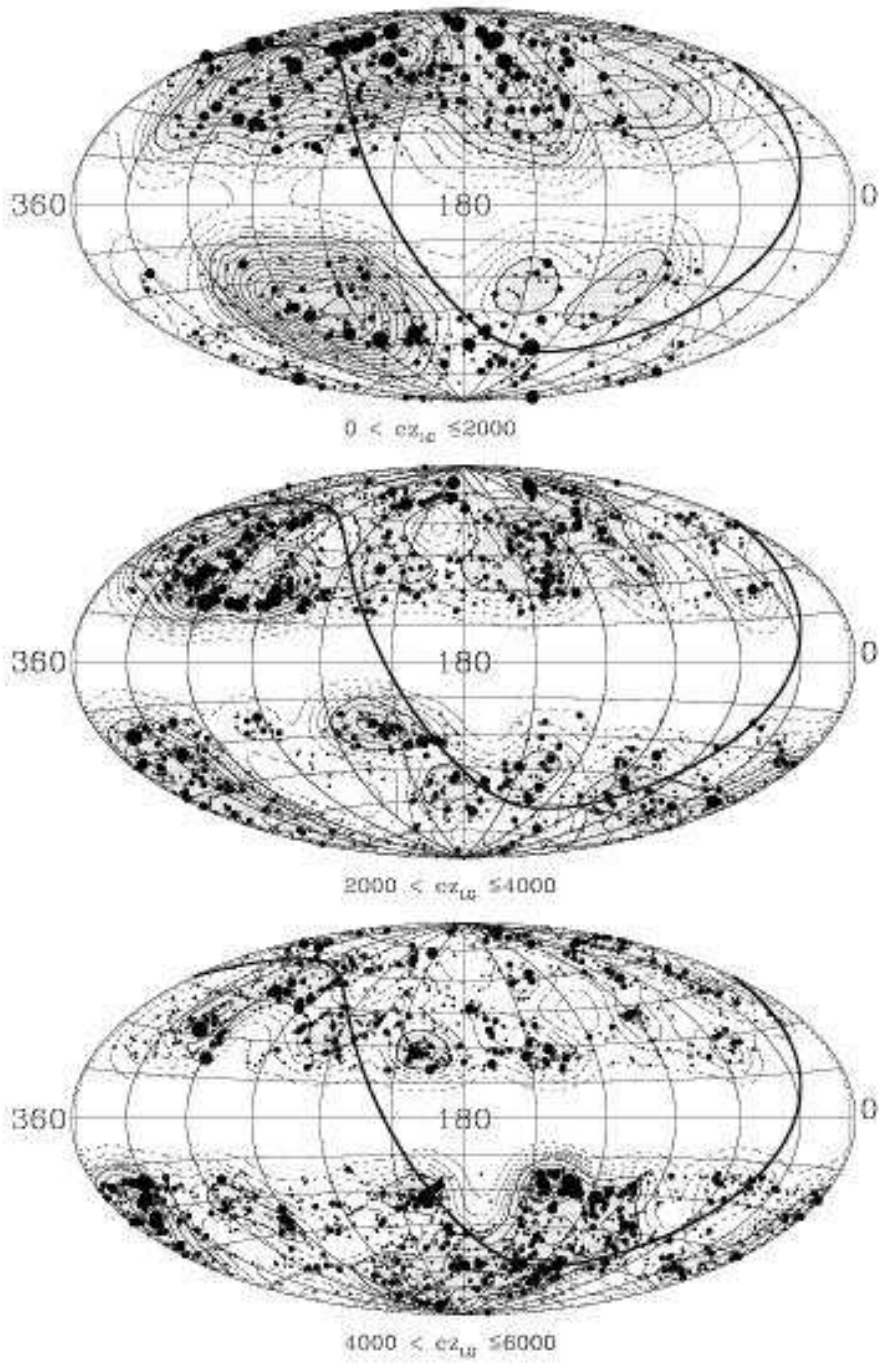

FIG. 1.— NOG galaxy systems reconstructed using the scaled *friends of friends* (P2) algorithm are shown in equal-area Aitoff projection on the sky using Galactic coordinates. The region devoid of galaxies is the zone of avoidance ($|b| < 20°$). The thick line is drawn at the celestial equator, $\delta = 0°$. Galaxy systems are indicated by filled circles, where the symbol size scales with the number of members of each groups. Also shown is the smoothed distribution of systems on shells at redshift 1000 km s^{-1}(upper), 3000 km s^{-1} (center), 5000 km s^{-1} (lower). Smoothing is performed in 3D with a variable Gaussian smoothing length given by the mean group separation (which is given by 309, 480 and 622 km s^{-1}respectively). The heavy contour denotes the mean density. Dashed contours represent densities below the mean (spaced with $\Delta(\frac{\delta n}{n}) = 0.2$ intervals). Regions in excess of the mean are in gray scale with contours spaced with $\Delta(\frac{\delta n}{n}) = 0.4$ intervals.

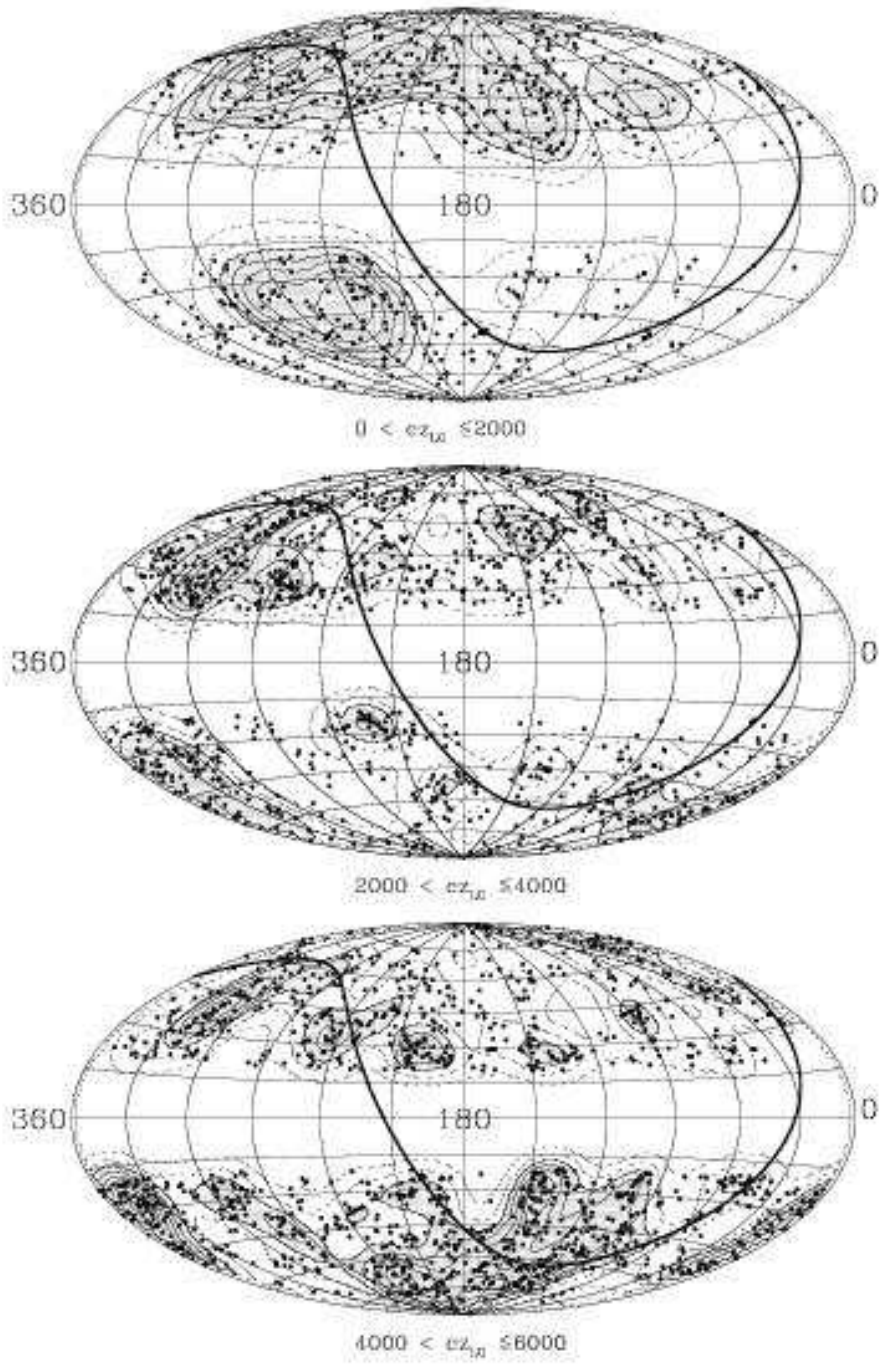

FIG. 2.— NOG isolated galaxies, i.e. galaxies left ungrouped after running the scaled friends of friends algorithm (P2), are shown in equal-area Aitoff projection on the sky using Galactic coordinates. The region devoid of galaxies is the zone of avoidance ($|b| < 20°$). The thick line is drawn at the celestial equator, $\delta = 0°$. Also shown is the smoothed distribution of systems on shells at redshift 1000 km s^{-1} (*upper*), 3000 km s^{-1} (*center*), 5000 km s^{-1} (*lower*). Smoothing is performed in 3D with a variable Gaussian smoothing length given by the mean group separation (which is given by 309, 480 and 622 km s^{-1} respectively). The heavy contour denotes the mean density. Dashed and solid contours represent densities below and above the mean and are spaced with $\Delta(\frac{\delta n}{n}) = 1/3$ intervals. Regions in excess of the mean are in gray scale.

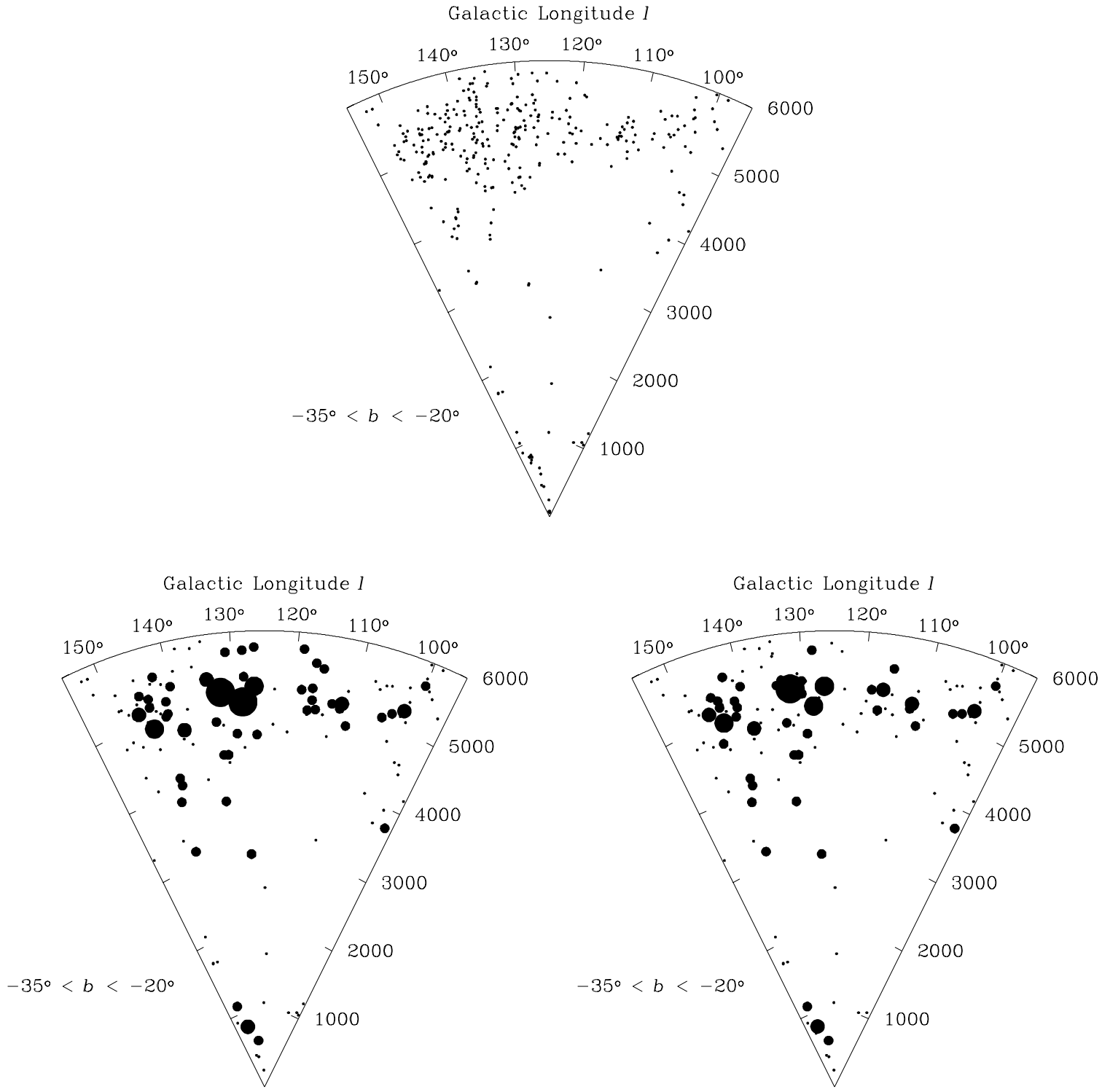

FIG. 3.— Cone diagrams of the distribution of NOG galaxies in the Perseus-Pisces region: the distance coordinate is the recession velocity (in the Local Group frame), angular coordinates is Galactic longitude (l). *Upper:*) distribution of galaxies before grouping; *Lower Left:*) distribution of objects after the application of the hierarchical (H) group-finding method; *Lower Right:*) distribution of objects after the application of the *friends of friends* (P1) group-finding algorithm. The same dot scaling as in Figure 1 is used to represent groups with different number of members.

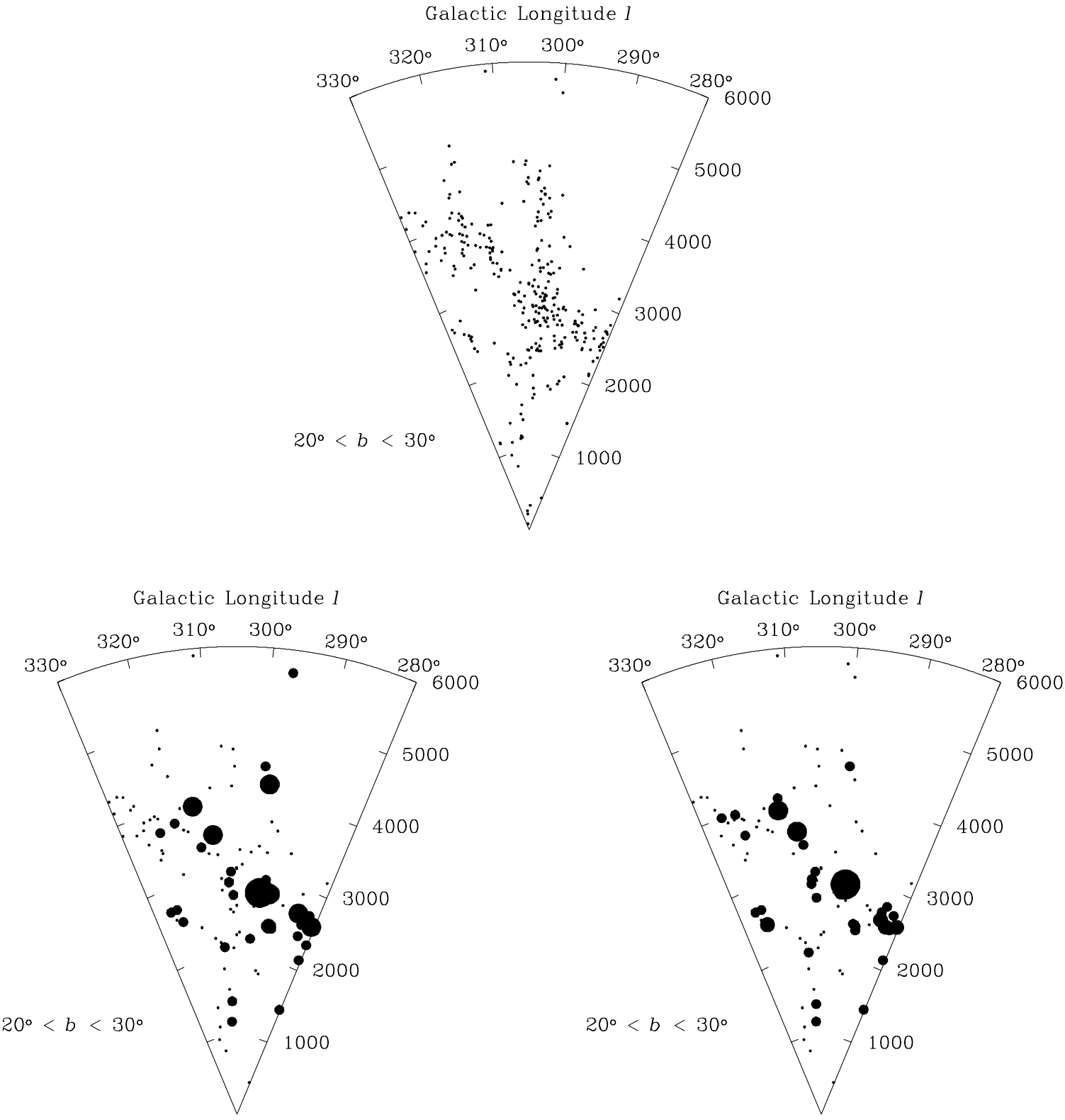

FIG. 4.— As in Figure 2 but for the Hydra-Centaurus region.

A comparison between Fig. 1 and Fig. 2 shows that groups delineate the same large-scale structures as do galaxies but with a different density contrast, i.e. groups are "biased" with respect to galaxies. In a separate paper (paper IV), we presented a detailed analysis of the clustering of NOG groups.

In Figures 3 and 4, we use cone diagrams in order to illustrate graphically the performance of two of our reconstruction algorithms (the H and P1 methods) in two interesting regions of the sky, the Perseus-Pisces and Hydra-Centaurus superclusters. These plots show that the different catalogs of groups have consistent spatial distribution. The top cone shows the ungrouped distribution of galaxies in redshift-space. Virialized systems show up as "Fingers of God" which are elongated along the observer's line of sight. Most groups as well as isolated galaxies are recovered by both methods. Moreover, these plots demonstrate how well our optimized grouping algorithms perform across a wide range of density enhancements and across the different large-scale structures in which the galaxies are embedded (i.e. orthogonal and parallel to the observer's line of sight).

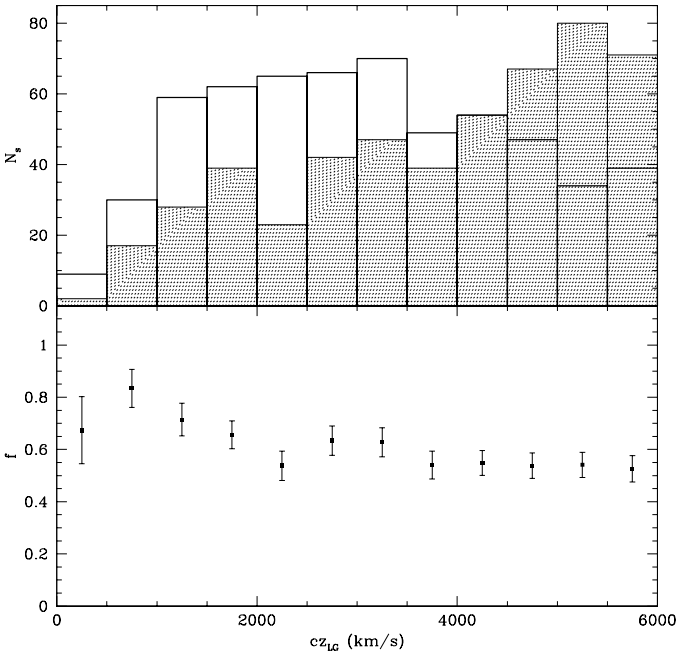

FIG. 5.— *Upper:* distribution of 1093 hierarchical binaries and groups as a function of distance in the northern and southern (shaded histograms) Galactic hemisphere. *Lower:* fraction of galaxies in hierarchical groups as a function of distance across the overall NOG volume. Data are binned in 500 km s^{-1} distance intervals.

Figure 5 illustrates that the fraction of NOG galaxies that are grouped is roughly a constant, independent of distance, although, due to large-scale clustering, the number of systems is an increasing function of distance in the southern galactic hemisphere and a decreasing one in the north. This indicates that, although we lose an increasing number of galaxies and groups with distance, due to the magnitude-limited sample, our group reconstruction methods do not suffer from any serious distance-dependent bias. Fig. 5 shows the results for H groups, but the other catalogs of groups give similar results.

3. THE LUMINOSITY FUNCTION OF VIRIALIZED SYSTEMS

The NOG groups are drawn from a magnitude-limited galaxy sample. In order to calculate the VSLF, we regard all systems as aggregates of galaxies much in the same way as galaxies are aggregates of stars. However, the crucial difference is that while galaxy fluxes can be directly measured with some device down to a limiting surface brightness, the flux of a system has to be inferred from members above a given apparent magnitude. When calculating the LF of galaxies, we must first correct for missing stars, which fall below the surface brightness limit, and then correct for the missing galaxies which fall below the magnitude limit of the catalog. In the same way, when constructing the LF of systems, we must first correct for missing galaxies (which fall below the magnitude limit of the survey) and then correct for missing systems.

We assume here that every system contains galaxies drawn from a universal galaxy LF, and thus has a large number of faint members. Consequently, even a single galaxy should be considered as the sole member observed above the apparent magnitude limit of a group, and thus requires a correction for unseen luminosity. By applying a luminosity correction to all systems, we obtain a "virialized systems" catalog. We stress that the result is fundamentally different from the group catalog from which it is derived. The group catalog suffers from the well-recognized problem that two groups with N visible elements identified (from a magnitude-limited galaxy sample) at two different distances correspond to potential wells of different masses. The systems catalog is more physical in the sense that it corresponds to halos with total absolute luminosity L.

To overcome these difficulties and estimate the luminosity function of systems, we must 1) assume a model describing how the missed galaxies are clustered around "seeds" defined by NOG systems, 2) check the photometric completeness of the resulting catalog in order to ensure that its luminosity distribution is representative of the group population and not only of our specific sample; 3) use a statistical estimator which is independent of density fluctuations because we know that groups tend to cluster at least as strongly as do galaxies (see Fig. 1).

3.1. *The Luminosity Selection Function*

We begin by introducing the statistical method used for estimation of the total luminosity $L_{\rm s}$ of systems.

The NOG galaxy LF, corrected for Malmquist bias and calculated after correcting for clustering is described by a Schechter-type function (Schechter 1976) with the following shape parameters: $\alpha_{\rm gal} = -1.10 \pm 0.03$, $M^*_{\rm gal} - 5\log h_{75} = -20.61 \pm 0.04$ (Marinoni 2001).

Marinoni (2001) also showed that the LF of galaxies *in* groups is marginally consistent with the field galaxy LF. Therefore, we assume that the observed luminosity in each bound system is a random realization of that portion of the universal LF $\phi(L)$ which lies above the local magnitude limit at the group distance, evaluated from the median redshift of its galaxy members. Specifically, $L_{\rm lim} = 10^{0.4(M_\odot - M_{\rm lim})} L_\odot$, where $M_\odot = +5.48$ mag and $M_{\rm lim} = m_{\rm lim} - 5\log\langle cz_{lg}\rangle - 15 + 5\log h_{75}$.

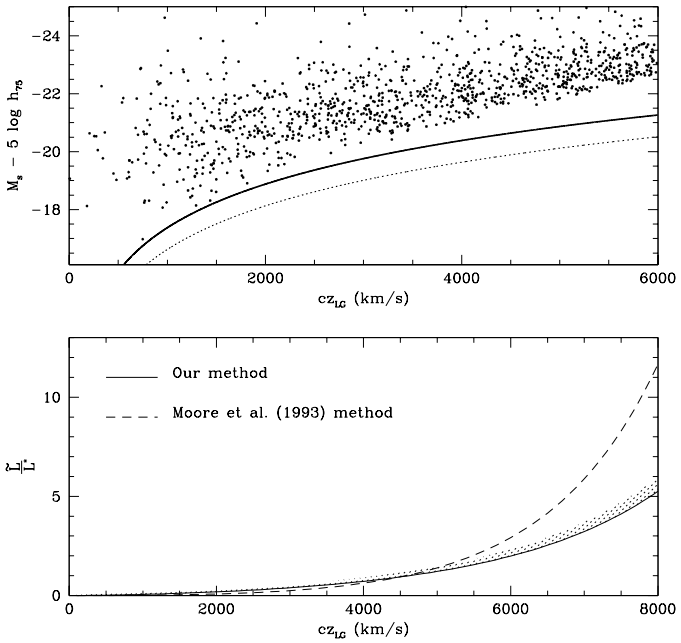

FIG. 6.— *Upper:* Spaenhauer diagram (Spaenhauer 1978) showing magnitude versus redshift for groups with $N \geq 2$ members. The absolute magnitude of the systems is the total one, i.e. corrected for unseen members. The solid line is the expected prediction for groups without any correction applied and corresponds to the following apparent variation in absolute magnitude $M_s = m_s^{lim} - 5\log\langle cz_{\rm LG}\rangle - 15 + 5\log h_{75}$ $(m_s^{lim} = 13.25)$. The dotted line is the visibility function of the NOG galaxy catalog and corresponds to an apparent magnitude cutoff $m_{\rm gal}^{lim} = 14$. *Lower:* The additive luminosity corrections per galaxy, in units of $L^*_{\rm gal}$ as given by our luminosity selection function is compared with the MFW method, using the magnitude system adopted in the NOG and the magnitude cut-off $m_{\rm gal}^{lim} = 14$. The hatched area shows how our luminosity selection function varies when it is computed using a power-law approximation at the faint end (M fainter than -16) with an exponent in the range from -1.1 to -1.8.

In order to recover the total number of galaxies in a system, the observed number density of galaxies is weighted by $w_N(r) = 1/S(r)$, where $S(r)$ is the selection function of a magnitude-limited sample (cf. eq. 4), yielding a corrected number density $n(r) = n_{\rm obs}(r)w_N(r)$. For luminosity, we can write the total expected luminosity of a system as

$$L_{\rm s}(r) = L_{\rm obs}(r) + \tilde{L}(r) = L_{\rm obs}(r)w_L(r) \qquad (5)$$

where $\tilde{L}$ denotes the unseen luminosity from galaxies below the magnitude limit , and $w_L(r)$ is the *luminosity-density weighting function* (see also Gourgoulhon, Chamaraux, & Fouqué 1992)

$$w_L = \frac{\int_0^\infty L\phi(L)dL}{\int_{L_{\rm lim}(r)}^\infty L\phi(L)dL}. \qquad (6)$$

As r goes to zero, the luminosity weighting function $w_L(r)$ reduces to 1 as desired. With this weighting scheme, we obtain an estimate of the absolute luminosity of groups which is independent of the magnitude limit of the catalog in which systems are identified, is independent of density fluctuations (i.e. independent of the LF normalization factor ϕ^*) and is less sensitive to the faint-end uncertainties and environmental dependencies of the galaxy LF.

There are other ways in which the total group light can be recovered. For example, MFW assumed the observed number of galaxies in each group to be a random sample of the observed portion of the LF and used an additive correction term of the form $\tilde{L} = N_{\rm obs}\int_0^{L_{\rm lim}(r)} L\phi(L)dL/(\int_{L_{\rm lim}(r)}^\infty \phi(L)dL)$.

Our correction and that of MFW are compared in Figure 6 where we plot the fractional expected correction in $L^*_{\rm gal}$ units as a function of distance for a single galaxy with luminosity $L^*_{\rm gal}$. Note that we do not expect these two corrections to be identical, since our correction is applied to the observed luminosity, whereas that of MFW is applied to the observed number.

We have tested our correction by moving nearby groups to progressively greater distances. However, at large distances our approach has the advantage that it depends very weakly on the adopted Schechter parameters because, at the faint end, the correction does not weight using the number density of dwarf galaxies, but using their luminosity density. (Note that our correction does not diverge using 0 as the lower limit of integration.) Thus, even if the galaxy function suffers some environmental dependence, i.e. becoming steeper at the faint end in clusters (Marzke & da Costa 1997), this correction is insensitive to this change. This can be seen explicitly in Figure 6, where we show the effect on our correction when we modify the faint-end behavior of the Schechter galaxy luminosity function by adding a power-law term with an exponent equal to -1.8 for luminosities fainter than $M = -16$ (see Zucca et al. 1997). The correction to the total system luminosity is small ($< 20\%$) and is not a strong function of distance. As noted above, we find a shallow slope (-1.1) for NOG galaxies and find no evidence for a large difference in the NOG B-band LF parameters for field galaxies versus galaxies in groups and clusters. Thus we can take the above correction as a conservative upper limit on such systematic effects.

3.2. *Sample Completeness*

We have applied eq. 6 to all systems, including isolated galaxies. This yields three "virialized system" (VS) catalogs of objects which, depending on the catalog of groups used, contain $\sim$ 4000 objects ($\sim$ 2800 systems with one observed member and $\sim$1100 groups with at least 2 members). For example, the hierarchical VS sample is composed by 2828 isolated galaxies and 1093 groups (with 4404 members) for a total of 3921 "systems". There are 691 binary systems, 297 systems with $3 \leq N < 5$ members and 195 systems with $N \geq 5$ members.

The large number of VS considered is not by itself a guarantee that our catalogs are photometrically complete. Instead, it is necessary to analyze the scaling of the number of systems as a function of the reconstructed magnitude and consider as suitable systems for the LF estimate only those for which the observed logarithmic scaling follows roughly the expected Euclidean $N_{\rm s} \propto 10^{0.6m_{\rm s}}$ behavior (no cosmological corrections are needed within the NOG volume). Each VS subsample (singles, binaries, etc.) has been analyzed with this method. As an example, in Figure 7, we plot integral and differential (independent bins) logarithmic counts for the sample of 195 hierarchical systems containing $N \geq 5$ members.

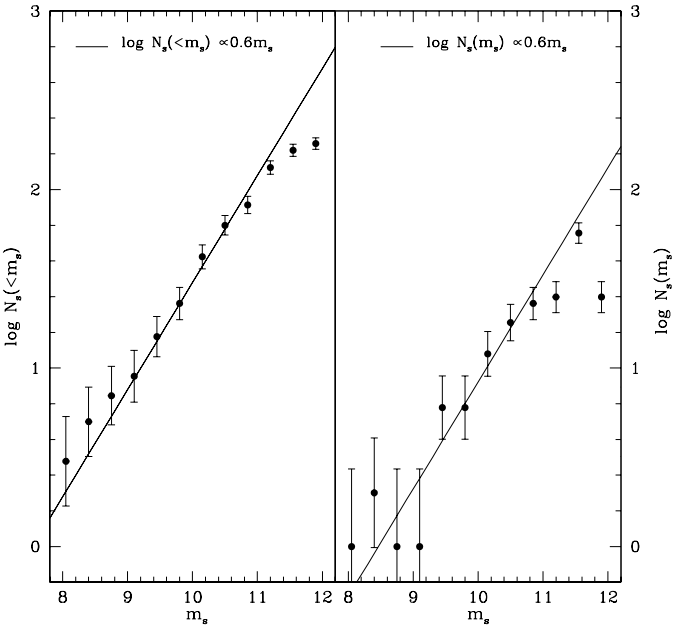

FIG. 7.— Integral (*left*) and differential (*right*) counts (binned in 0.4 magnitude intervals) for NOG groups with $N_{\rm gal} \geq 5$ members. Apparent magnitudes have been corrected with the luminosity selection function. Bars represent $\pm 1\sigma$ Poisson errors. Solid lines indicate the expected prediction in a volume with an Euclidean geometry and a homogeneous distribution of systems.

The Euclidean growth rate is followed over a range of 3 magnitudes and breaks down at $B \sim 11.1$ mag. Roughly the same behavior (but with different limits of completeness) is observed in different subsamples of the same VS catalog or different VS catalogs. The magnitude limits of completeness and the number of objects which meet these criteria are reported in Table 1 for the case of the H groups. Although this selection reduces the number of systems available for the analysis, systematic errors due to incompleteness are avoided.

3.3. *Results*

In recovering the LF shape and normalization for various group subsamples, we have used the estimation technique adopted in Paper II. In particular, the shape has been derived through Turner's (1979) method and the normalization has been calculated using the relation $\phi^*_{\rm s} = n_{\rm s} / \int_{-\infty}^{M_c} \phi(M_{\rm s}) dM_{\rm s}$ with $M_c = m_{\rm s}^{lim} - 5\log 500 - 15 + 5\log h_{75}$, and where $m_{\rm s}^{lim}$ is the limiting apparent magnitude of completeness of each subsample and $n_{\rm s}$ has been determined using the minimum variance estimator of Davis & Huchra (1982).

Our estimate of the VSLF is shown in Figure 8 for the H and P1 VS samples. We have found that a Schechter function with parameters $\alpha_{\rm s} = -1.4 \pm 0.03$, $M^*_{\rm s} - 5\log h_{75} = -23.1 \pm 0.06$ and $\phi^*_{\rm s} = 4.8 \times 10^{-4}\ h^3_{75}\,{\rm Mpc}^{-3}$ provides a good fit to data over a broad range of absolute luminosity ($-24.5 \leq M_{\rm s} - 5\,log\,h_{75} \leq -18.5$). In Figure 8 we also show the joint distribution of errors in $\alpha_{\rm s}$ and $M^*_{\rm s}$ as derived from the χ^2 matrices of the least squares fit.

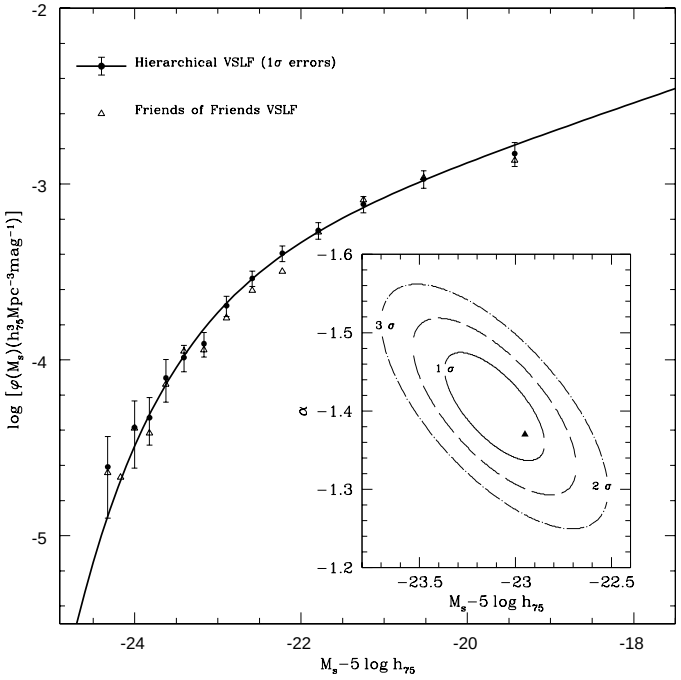

FIG. 8.— The virialized systems luminosity function (differential form) as derived using NOG hierarchical (H) (solid circles together with $\pm 1\sigma$ error bars) and *friends of friends* (P1) (open triangles) group catalogs. The best fitting Schechter LF function (solid line) and the 1, 2, 3 σ confidence ellipses are also shown. The solid triangle represents in the $(\alpha_{\rm s} - M^*_{\rm s})$ space the best-fitting Schechter parameters of the *friends of friends* LF.

Figure 8 also shows that different catalogs of groups (H and P1) do not give significantly different LFs. Moreover, since the P2 groups (obtained by varying the velocity linking parameter) give a LF which is very similar to the LF obtained from the P1 groups in which the velocity link parameter is kept fixed, we argue that while other group properties (e.g. velocity dispersion) considerably depend on the values chosen for this parameter (e.g. Trasarti-Battistoni 1998), the LF is rather stable and only weakly sensitive to different choices. Besides we can use redshifts as distance indicators and obtain a VSLF which is not different from a LF that would be obtained in a pseudo-real space analysis. For the sake of simplicity, in the following we shall present results obtained using the H groups.

While the LF is rather insensitive to the group-finding algorithm, it is somewhat sensitive to the choice of density threshold. If thresholds are set much higher than the ones used in this paper, this yields a larger proportion of field galaxies and, hence, to a steeper faint-end of the LF, in agreement with the results of MFW. Marinoni & Hudson (2001) show that our adopted density thresholds lead to systems which are virialized.

In Figure 9 we show that the VSLF can be economically described in terms of a smoothly decreasing double-power law of the following form

$$\phi(L_{\rm s})dL_{\rm s} = \begin{cases} \phi_{\rm pl}\left(\frac{L_{\rm s}}{L_{\rm pl}}\right)^{-1.45\pm0.07} d(\frac{L_{\rm s}}{L_{\rm pl}}) & \text{if} \quad L_{\rm s} < L_{\rm pl} \\ \phi_{\rm pl}\left(\frac{L_{\rm s}}{L_{\rm pl}}\right)^{-2.35\pm0.15} d(\frac{L_{\rm s}}{L_{\rm pl}}) & \text{if} \quad L_{\rm s} \geq L_{\rm pl} \end{cases} \tag{7}$$

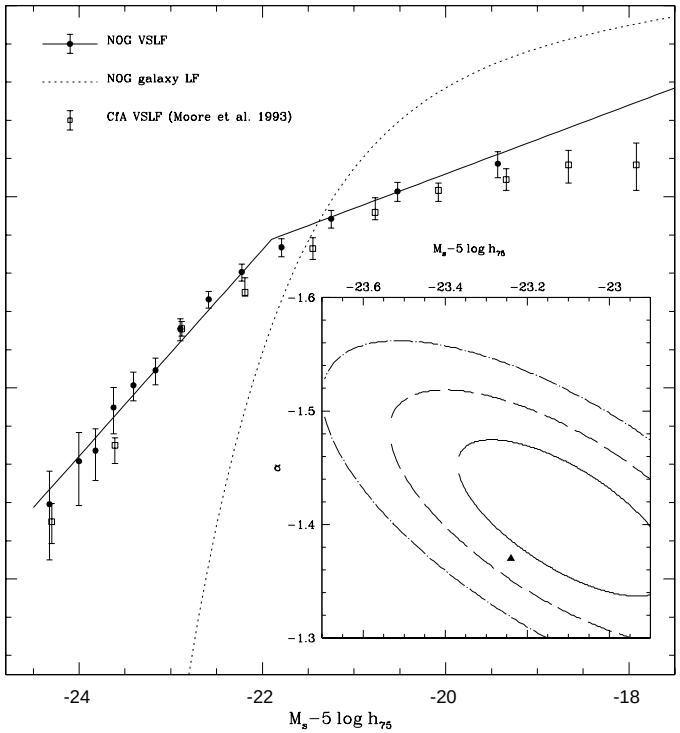

FIG. 9.— The VS luminosity function is plotted (solid circles) and compared to the CfA VSLF of MFW (squares) and to the NOG galaxy LF (dotted line). Solid lines represent a double power law fit to data. The 1, 2, 3 σ confidence ellipses of the best fitting Schechter LF are also shown. The solid triangle represents in the $(\alpha_s - M_s^*)$ space the best-fitting Schechter parameters of the CfA group LF as given by MFW (after having transformed Zwicky magnitudes into the B system used in the NOG).

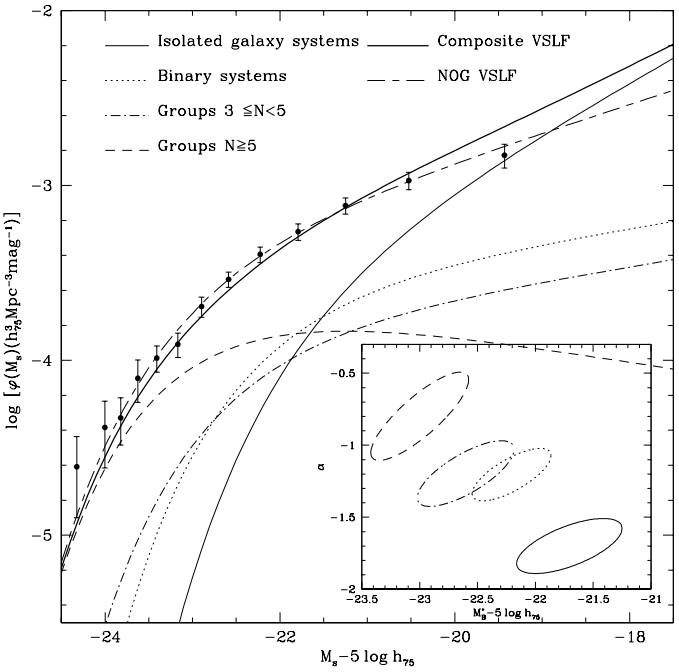

FIG. 10.— Composite group LF obtained by summing the contribution from halos hosting visible systems of different richness. Points represent the VSLF. The corresponding 1 σ error ellipses are plotted in the inset.

where $L_{\rm pl} = 8.5 \times 10^{10} h_{75}^{-2} L_\odot$, corresponding to $M_{\rm pl} = -21.85$ and $\phi_{\rm pl} = 6.5 \times 10^{-4}\ h_{75}^3\,{\rm Mpc}^{-3}$. In contrast with the galaxy LF, which has a sharp break at $L^*_{\rm gal}$, the VSLF shows a more slowly-varying behavior. In the limit of low luminosities, the VSLF approaches the NOG galaxy LF as expected, since these "systems" are single field dwarf galaxies.

The global mean density of the VS distribution is $n \sim 2.2 \times 10^{-2} h_{75}^3\,{\rm Mpc}^{-3}$ for systems with a magnitude brighter than $M_{\rm s} - 5\log h_{75} = -15$ and $n \sim 6.2 \times 10^{-3} h_{75}^3\,{\rm Mpc}^{-3}$ for systems brighter than $M_{\rm s} - 5\log h_{75} = -18$.

In Figure 9, we also show the good agreement ($< 2\sigma$) between the CfA groups LF and the NOG VSLF. In order to compare our results (which use the corrected B total magnitude in the RC3 system) to the results of MFW (which are based on the Zwicky magnitude system, B_z), we have made the following transformations: $B - B_z = -0.35$ mag (Auman et al. 1989) and $B_{(corr)} - B = -0.25$ mag (for the internal absorption, see Paper II).

The two volumes are largely independent, with NOG being shallower and wider in area than the CfA1 volume studied by MFW. The agreement between the two VSLFs is reassuring because the CfA groups have been identified using a variant of the P algorithm with different selection parameters and scaling laws, as well as a different luminosity correction and a different method for estimating the LF.

Moreover, if we consider the GT VSLF, we see that their bright-end slope has a power-law behavior ($L_{\rm s}^{-7/3}$) with essentially the same slope of our LF. However, due the lack of small systems with low surface density enhancement with respect to the background, their data show a faint end which is flatter than our LF and that of MFW. Our results are in marginal agreement with the LF derived by Bahcall (1979) who finds a significantly flatter slope ($\sim 3\sigma$) at the faint end.

In Figure 10, we have estimated the LF for different range of group richness from isolated galaxies to groups with N$\geq$ 5 members. The best-fit parameters are given in Table 1. While field galaxies dominate the low-luminosity portion of the VSLF, richer systems contribute in a progressive way to the bright end of the VS LF. We also show the total LF defined as the sum over the LFs pertaining to different samples.

The remarkable flatness of the luminosity-weighted VSLF was first noted by GT. A significant contribution to the total luminosity density of the universe is made by both small and large systems (see Figure 11). The characteristic luminosity of the NOG *galaxy* LF is $L^*_{\rm gal} = 2.7 \times 10^{10} h_{75}^{-2} L_\odot$ We find that after correcting for the unseen luminosity, systems with total luminosity $L_{\rm s} < L^*_{\rm gal}$ make up 25% of the total luminosity density ρ_L of the universe, systems with $L_{\rm s} < 5L^*_{\rm gal}$ and $L_{\rm s} < 10L^*_{\rm gal}$ contribute by 58% and 75% respectively, while a substantial fraction of luminosity density (10%) is contributed by large systems with more than $30L^*_{\rm gal}$.

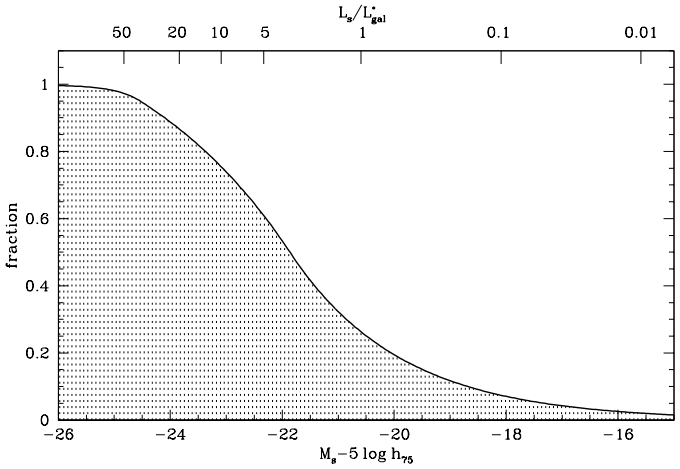

FIG. 11.— Fraction of the total luminosity density from systems with $L < L_{\rm s}$ as derived from the VSLF. $L^*_{\rm gal}$ is the characteristic luminosity of the NOG galaxy LF ($M^*_{\rm gal} - 5\log h_{75} = -20.61$) while $L_{\rm s}$ ($M_{\rm s}$) is the absolute luminosity of galaxy systems.

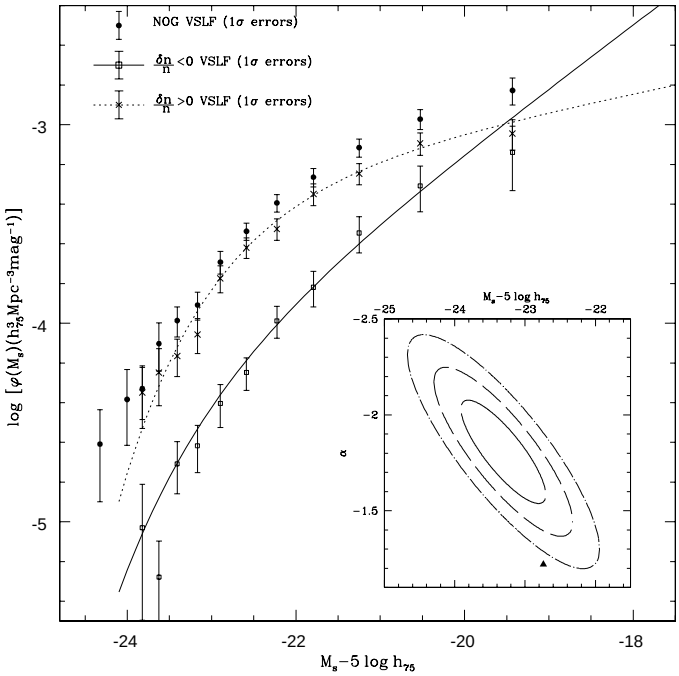

FIG. 12.— The VS luminosity function for hierarchical systems in regions of different density. The environmental density parameter $\frac{\delta n}{n}$ for each halo has been weighted using a Gaussian filter (eq. 3) with a fixed smoothing length $R_{\rm s} = 530$ km s^{-1} which corresponds to the NOG mean inter-group separation. The inset shows the 1, 2, 3 σ contours for the joint distribution of errors of the Schechter parameters $(\alpha_{\rm s}, M^*_{\rm s})$ of systems in low density regions. The solid triangle represents in the $(\alpha_{\rm s} - M^*_{\rm s})$ space the best-fitting Schechter parameters of the LF of systems in high density regions.

3.4. *Environmental Effects on the Luminosity Function of Virialized Systems*

The mass function of dark matter halos is expected to show a dependence on the large-scale environment, as predicted by e.g. Mo & White (1996) using an extension of the Press-Schecter formalism, and confirmed in N-body cold dark matter simulations (see also Lemson & Kauffmann 1999). The sense of the predicted trend is that dark matter halos in overdense regions should be biased toward the high masses than those forming in lower density regions. Note that the extended Press-Schecter theory makes predictions for the clustering of virialized dark matter halos, which are typically groups or clusters rather than individual galaxies.

Many workers have looked for such an effect by studying the luminosities of *galaxies* as a function of environment, with conflicting results (e.g., Valotto et al. 1997; López-Cruz et al. 1997; Bromley et al. 1998; Ramella et al. 1999; Zabludoff & Mulchaey 2000; Christlein 2000; Balogh et al. 2001). Part of this may be due to different bandpasses used in different studies, the environmental dependence being strong in the K-band (e.g. Balogh et al 2001) and weak in the B-band. Marinoni (2001) compared NOG galaxies in regions of high density contrast to those in low density contrast, and also compared isolated galaxies to members of systems. He found that the B-band luminosity function of galaxies as well as the luminosity functions of early and late morphological types are consistent with no dependence on environment, although a weak trend (differences in M_* of a few tenths of a magnitude) is also permitted by the data.

It is clear that at the very bright end, more luminous galaxies are more strongly clustered (Norberg et al. 2001), and hence one should expect some dependence of the LF on environment. The trend found by Norberg et al, while highly significant, is rather weak: the biasing parameter $b/b_* = 0.85 + 0.15L/L_*$, where b_* is the biasing parameter of an L_* galaxy.

Thus at a magnitude brighter than $L*$, the relative biasing is only 1.22. This leads to a rather weak effect of when comparing, for example, Schecter function parameters in overdense and underdense regions.

In contrast to the situation for individual galaxies, we expect that the total luminosities of virialized systems are closely related to the dark matter content of the virialized halo. Systems should therefore be expected to display the environmental dependence predicted by the extended Press-Schecter theory. We can test this prediction as follows. We assign to each system an environmental density parameter ($\frac{\delta n}{n}$) computed by smoothing the data with a Gaussian filter (eq. 3) of fixed smoothing length $R_{\rm s} = 530$ km s^{-1} (which corresponds to the mean NOG inter-group separation). Systems which lie in underdense regions ($\frac{\delta n}{n} < 0$; 361 objects) and overdense regions ($\frac{\delta n}{n} > 0$; 946 objects) are differently distributed in luminosity. Note that the system in question is excluded from the smoothed density estimate.

Figure 12 shows that the hierarchical VSLF is sensitive to the large-scale environmental density: the luminosity distribution of halos which inhabit low density regions is biased toward faint magnitudes.

Both the distributions are well described in term of a Schechter function with parameters [-1.8,-23.3] and [-1.2, -22.7] respectively in low and high density regions. The difference in Shechter function parameters is significant at the 3σ level. A signal of the same type is also present, al-

beit at a marginal (1.5σ) significance level when we smooth the halo density field on a larger scale ($R_{\rm s} = 1000 {\rm km\ s^{-1}}$).

Thus, in contrast to the situation for galaxies, the VSLF is clearly dependent on the large-scale environment. This effect is not the result of the rather weak dependence of B-band galaxy LFs on environment. More luminous, and presumably more massive, systems are more abundant in high-density regions and hence are more strongly clustered, in agreement with the group correlation function results of Paper IV. One astrophysical implication of this result is that the higher relative biasing of early-type galaxies is then a byproduct of the environmental dependence of virialized halos coupled with the morphology-density relation.

4. SUMMARY AND CONCLUSIONS

The traditional approach has been to classify non-linear structures as being either galaxies, groups or clusters. In contrast to either galaxies or rich clusters of galaxies, however, groups have received little attention in the literature, despite the fact that they these virialized objects contain most of the luminosity, and hence presumably most of the mass, in the universe. Our approach has been to treat all virialized "systems", from isolated single galaxies to rich clusters of galaxies, as a continuum, and to consider the total optical luminosity of these systems.

We have analyzed the NOG group catalog (Paper III) in order to correct the total B-band luminosities of these systems for the luminosity of galaxies below the magnitude limit of the sample and for the completeness of subsamples of the group catalog, and have used this to measure the luminosity function of virialized systems. We verify that the luminosity function is insensitive the choice of the group-finding algorithm. It is also insensitive to the value of the velocity link parameter adopted in the percolation algorithm, whereas it is somewhat sensitive (at the faint end) to the density contrast at which groups are defined. Our luminosity function is in good agreement with that of MFW, who used a quite different approach to its determination and relied on groups identified in the CfA1 survey.

The luminosity function of virialized systems is well described by a double-power law, $\phi(L_{\rm s})dL_{\rm s} \propto L_{\rm s}^{-1.45\pm0.07}dL$ for $L_{\rm s} < L_{\rm s}^*$ and $\phi(L_{\rm s})dL_{\rm s} \propto L_{\rm s}^{-2.35\pm0.15}dL_{\rm s}$ for $L_{\rm s} > L_{\rm s}^*$ with $L_{\rm s}^* = 8.5 \times 10^{10} h_{75}^{-2} L_\odot$, over a broad range of absolute luminosity ($-24.5 \leq M_{\rm s} - 5\log h_{75} \leq -18.5$). Our results indicate that 25%, 50%, and 75% of the luminosity of the universe is generated in systems with $L_{\rm s} < L_{\rm gal}^*$, $L_{\rm s} < 2.9 L_{\rm gal}^*$ and $L_{\rm s} < 10 L_{\rm gal}^*$, respectively; 10% of the overall luminosity density is supplied by systems with $L_{\rm s} > 30 L_{\rm gal}^*$.

Finally, we find that the luminosity function of systems depends on the large-scale environment, in the sense that halos distributed in low-density regions host preferentially low-luminosity systems, while there is an excess of bright virialized systems in high-density regions.

CM would like to acknowledge his Ph.D. adviser GG, to whom this paper is dedicated, for his constant help and guidance during this project. He will be missed.

We also wish to thank C.M. Baugh, A.J. Benson, M. Davis, R. Giovanelli, M. Haynes, M. Mezzetti and P. Monaco for interesting conversations. This work has been partially supported by the Italian Ministry of University, Scientific and Technological Research (MURST) and by the Italian Space Agency (ASI). MJH acknowledges support from the NSERC of Canada.

REFERENCES

Abell, G. O. 1958, ApJS, 3, 211
Auman, J. R., Hickson, P., & Fahlmann, G. G. 1989, PASP, 101, 859
Bahcall, N. A. 1979, ApJ, 232, 689
Balogh, M., Christlein, D., Zabludoff, A., & Zaritsky, D. 2001, astro-ph/0104042
Bromley, B. C., Press, W, H., Lin, H., & Kirschner, R. P. 1998, ApJ, 505, 25
Christlein, D. 2000, ApJ, 545, 145
Davis, M., & Huchra, J. 1982, ApJ, 254, 437
Davis, M., Huchra, J., Latham, D. W., & Tonry, J. 1982, ApJ, 253, 423
de Vaucouleurs, G., de Vaucouleurs, A., Corwin, H. G., Buta, R. J., Paturel, G., & Fouqué, P. 1991, Third Reference Catalogue of Bright Galaxies, 9th version
Gaidos, E. J. 1997, AJ,113, 117
Giuricin, G., Marinoni, C., Ceriani, L., & Pisani, A. 2000, ApJ, 543, 178 (Paper III).
Giuricin, G., Samurovic, S., Girardi, M., Mezzetti, M., Marinoni, C. 2001, ApJ, 554, 857 (Paper IV)
Gott, J. R., & Turner E. L. 1977, ApJ, 216, 357
Gourgoulhon, E., Chamaraux, P., & Fouqué, P. 1992, A&A, 255, 69
Huchra, J. P., & Geller, M. 1982, ApJ, 257, 423
Huchra, J. P., Davis, M., Latham D. W., & Tonry, J. 1983, ApJS, 53, 89
Iovino, A., Giovanelli, R., Haynes, M., Chincarini, G., & Guzzo, L. 1993, MNRAS, 265, 21
Lemson, G., & Kauffmann, G., 1999, MNRAS, 286, 795
Lopez-Cruz, O. 1997, University of Toronto
Lumsden, S. L., Collins, C. A.,Nichol, R, C., Eke, V. R., & Guzzo, L. 1997, MNRAS, 290, 119
Marinoni, C., Monaco, P., Giuricin, G., & Costantini, B. 1998, ApJ, 505, 484 (Paper I)
Marinoni, C., Monaco, P., Giuricin, G., & Costantini, B. 1999, ApJ, 521, 50 (Paper II)
Marinoni, C. 2001, Ph.D. Thesis, University of Trieste
Marinoni, C., & Hudson, M. J. 2001, ApJ, submitted (Paper VI)
Marzke, R. O., & da Costa, L. N. 1997, AJ, 113, 185
Materne, J. 1978, A&A, 63, 401
Mo, H. J., & White, S. D. M., 1996, MNRAS, 282, 347
Moore, B., Frenk, C. S., & White S. D. M. 1993, MNRAS, 261, 827
Nolthenius, R., & White, S. D. M. 1987, MNRAS, 235, 505
Norberg, P., et al. 2001, MNRAS, submitted, astro-ph/0105500
Ramella, M., et al. 1999, A&A, 342, 1
Rauzy, S., Adami, C., & Mazure. A. 1998, A&A, 337, 31
Schechter, P. 1976, ApJ, 203, 297
Spaenhauer, A. M. 1978, A&A, 313, 65
Trasarti–Battistoni, R. 1998, A&AS, 130, 341
Tully, R. B. 1980, ApJ, 237, 390
Turner, E. L. 1979, ApJ, 231, 645
Valotto, C. A., Nicotra, M. A., Muriel, H., & Lambas, D. G. 1997 ApJ, 481, 594
Zabludoff, A.I. & Mulchaey, J. S. 2000, ApJ, 539, 136.
Zucca, E. et al. 1997, A&A, 326, 342

TABLE 1
LUMINOSITY FUNCTION PARAMETERS FOR VARIOUS SAMPLES OF SYSTEMS

	All systems	Isolated galaxy "systems"	Binary systems	Groups $3 \leq N_g < 5$	Groups $N_g \geq 5$
$m_{\rm lim}$	12.	12.	12.	11.5	11.1
$N_{\rm s}$	1307	377	450	247	187
$V/V_{\rm max}$	0.47	0.61	0.54	0.49	0.31
α	-1.40 ± 0.03	-1.7 ± 0.12	-1.2 ± 0.12	-1.2 ± 0.15	-0.8 ± 0.20
$M_B^* - 5 \log h_{75}$	-23.1 ± 0.06	-21.7 ± 0.30	-22.2 ± 0.22	-22.6 ± 0.27	-23.0 ± 0.28
$\phi^*(10^{-4} h_{75}^3\ {\rm Mpc}^{-3})$	4.8	3.9	2.9	1.6	2.7
$\rho_L(10^8 L_\odot h_{75}^3\ {\rm Mpc}^{-3})$	2.0	0.86	0.39	0.32	0.59